



Platinum complexes with pyrimidine-functionalized N-heterocyclic carbene ligands – Synthesis and solid state structures

Dirk Meyer, Alexander Zeller, Thomas Strassner*

Physikalische Organische Chemie, Technische Universität Dresden, Bergstrasse 66, 01062 Dresden, Germany

ARTICLE INFO

Article history:

Received 11 November 2011

Received in revised form

9 December 2011

Accepted 12 December 2011

Keywords:

Platinum

N-Heterocyclic carbene

Catalysis

Solid state structure

ABSTRACT

The ligands of the two most successful systems described in the literature for the activation and functionalization of methane have been merged and a series of novel pyrimidine functionalized platinum(II)(NHC) complexes with aryl and alkyl substituents [1-(2-Pyrimidyl)-3-(aryl or alkyl)imidazoline-2-ylidene platinum(II) chlorides] was synthesized by transmetalation via the corresponding silver complexes. All compounds have been fully characterized by ^1H and ^{13}C -NMR spectroscopy, elemental analysis, and with five X-ray single crystal structures. As for the related palladium(II) complexes in most cases we observed structures of the type $[\text{Pt}(\text{L})\text{Cl}_2]$, while for the sterically less demanding methyl substituent a complex is formed, where two ligands are coordinated to one metal center $[\text{Pt}(\text{L})_2\text{Cl}]^+$.

© 2011 Elsevier B.V. All rights reserved.

1. Introduction

One of the most prominent and successful systems for the catalytic methane activation is a platinum(II) complex with a bipyrimidine ligand where the metal is stabilized by a bidentate coordination of two nitrogen atoms [1]. Based on quantum chemical calculations it was claimed that the nitrogen atom functions as an acceptor for protons in the strongly acidic reaction mixture (oleum) [2,3]. Other active catalysts are based on chelating biscarbene palladium(II) systems like the 1,1'-dimethyl-3,3'-methylenediimidazolin-2,2'-ylidene-palladium(II) bromide which have been developed by our group [4]. They donate significantly stronger through the two carbene carbon atoms and can therefore stabilize the metal even better.

We recently demonstrated that [1-(2-pyrimidyl)-3-(aryl or alkyl)-imidazoline-2-ylidene palladium(II)] complexes $[(\text{pym})^{\wedge}(\text{NHC-R})\text{Pd}^{\text{II}}\text{Cl}_2]$ are also active in the methane activation. The ligand can be considered as a mixture of the two well known systems (Scheme 1) [5]. The palladium catalysts prepared were active in the methane activation reaction under the reaction conditions established in the group (trifluoroacetic acid and –anhydride, 30 bar methane, 90 °C), but didn't show any significant benefit compared to the known biscarbene systems. We therefore were interested whether the corresponding Pt(II) complexes $[(\text{pym})^{\wedge}(\text{NHC-R})\text{Pt}^{\text{II}}\text{Cl}_2]$ might be more active [6,7].

We present the synthesis of the corresponding platinum(II) complexes which constitute the other possible combination of the

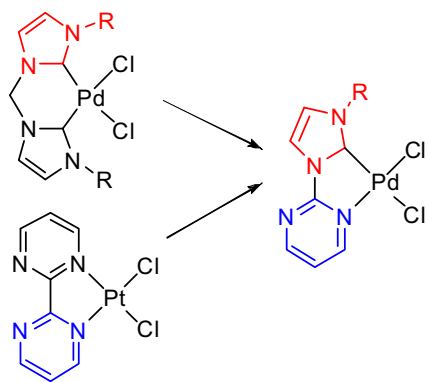
Periana (bipyrimidine-) and Strassner (biscarbene-) systems. Compared to the Periana system the pyrimidine–NHC–ligands donate additional electron density and coordinate to the metal through one nitrogen atom which has recently been demonstrated with various metals [8–17]. The pyrimidine–NHC–ligands can also get protonated at the second nitrogen atom, combining the advantages of both catalytically active systems. Chen and coworkers have even been successful in using metal powders [18] or recently electrolysis for the direct synthesis of the metal complexes [19].

Parallel to our work two platinum(II) complexes of 1-(2-pyrimidyl)-3-(aryl or alkyl)imidazol-2-ylidene (aryl: 2,4,6-trimethylphenyl; alkyl: methyl) have recently been published, but in these cases with a ligand/metal ratio of 2:1 [15,20]. In the past years, it was shown that Pt(II) complexes of bis(NHC) ligands are active catalysts of the methane activation under the same conditions established for their Pd(II) derivatives but are less stable and therefore show lower turnover numbers (TON) [21,22]. Through the introduction of aromatic substituents the stability of the complexes could be increased [21] and we therefore decided to synthesize alkyl as well as aryl substituted [1-(2-pyrimidyl)-3-imidazol-2-ylidene platinum(II)] complexes.

2. Results and discussion

The imidazolium salts 1-(2-pyrimidyl)-3-(2,6-diisopropylphenyl)imidazolium chloride **1** and 1-(2-pyrimidyl)-3-(2,4,6-trimethylphenyl)imidazolium chloride **2** are accessible by the reaction of the N-substituted imidazole with 2-chloropyrimidine in good yields.

* Corresponding author. Tel.: +49 351 46338571; fax: +49 351 46339679.
E-mail address: thomas.strassner@chemie.tu-dresden.de (T. Strassner).



Scheme 1. Catalytically active systems in the conversion of methane.

Running the reaction neat in an ACE pressure tube at 80 °C lead to significantly better yields. The structure of **1** shows that the pyrimidin ring is almost in plane with the imidazole core while the bulky isopropyl substituents in 2,6-position of the aryl ring lead to an orthogonal geometry of the aryl ring (Fig. 1).

Reaction of the imidazolium salts with Ag₂O in dichloromethane leads to the corresponding silver(I) salts in good yields [5]. We were able to get single crystals of **3** suitable for X-ray diffraction (Fig. 2).

The C1–Ag–Cl angle of 174.3(1)° confirms the almost linear coordination of the silver atom. The pyrimidine and the imidazole ring are twisted by –23.2(2)° (C1–N1–C4–N3), while the 2,6-disubstituted ring remained orthogonal (C1–C2–C8–C9 –87.7(2)°). The aryl substituted platinum complexes [(pym)⁺(NHC-DIPP)Pt^{II}Cl₂] **5** (Fig. 3) and [(pym)⁺(NHC-Mes)Pt^{II}Cl₂] **6** (Fig. 4) have been synthesized by transmetalation of the corresponding silver complexes [5] [(pym)⁺(NHC-DIPP)AgCl] **3** and [(pym)⁺(NHC-Mes)AgCl] **4** with [(COD)Pt^{II}Cl₂] [23] (Scheme 2).

The platinum(II) complexes have been fully characterized by NMR spectroscopy, elemental analysis and solid state structures (Figs. 3 and 4). Complex **6** crystallized with one molecule acetonitrile as **6**·CH₃CN.

It is interesting to note that **6**·CH₃CN in our hands crystallizes in a different geometry compared to what had been observed before. But in our case we also did not observe the formation of the AgCl₂ counterion, probably due to the lower solubility in CH₂Cl₂,

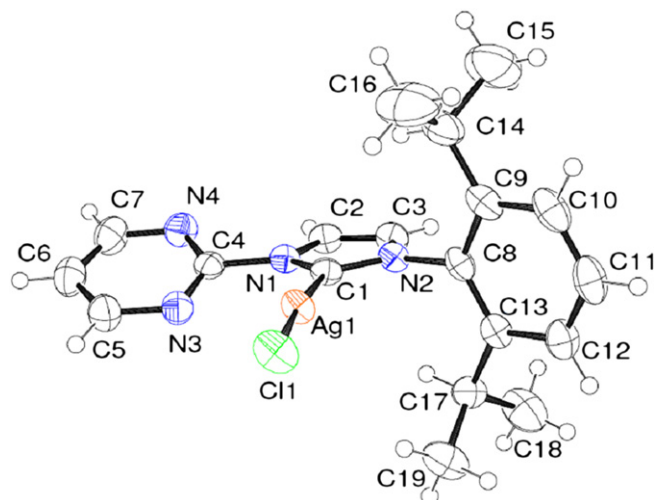


Fig. 2. ORTEP style plot of **3** in the solid state. Thermal ellipsoids are drawn at the 50% probability level. Selected bond lengths (Å) and angles (°): Ag1–C1 2.072(2), Ag1–Cl1 2.321(1), Ag1–N3 3.082(2), C1–Ag1–N3 62.8(1), C1–Ag1–Cl1 174.3(1), C1–N1–C4–N3 –23.2(2), C1–N2–C8–C9 –87.7(2).

compared to CH₃CN used in Ref. [15]. Therefore the formation of the 1:1 vs. 2:1 complexes seems to be more dependent on the reaction conditions than on the steric demand of the aryl/alkyl substituent in the 3-position of the imidazole. The solid state structure of complex **6**·CH₃CN shows similar bond lengths and angles as the corresponding Pd(II) complex [5]. The main difference between the two Pt(II) complexes **5** and **6**·CH₃CN is the angle between the aryl substituent and the plane of the ligand. In case of the very bulky 2,6-diisopropylphenyl substituent in **5** the torsional angle between the phenyl ring and the plane of the imidazol ring is nearly 90° while in case of the 2,4,6-trimethylphenyl substituted complex **6**·CH₃CN the aryl substituent is more in plane by almost 30°. The steric demand of the 2,6-diisopropylphenyl substituent seems to be responsible for the orthogonal arrangement as the corresponding torsional angle (C1–N2–C8–C9) is around 90° in the imidazolium precursor **1** as well as in the silver complex **3**. As expected, the platinum is in a nearly perfect square-planar coordination in both

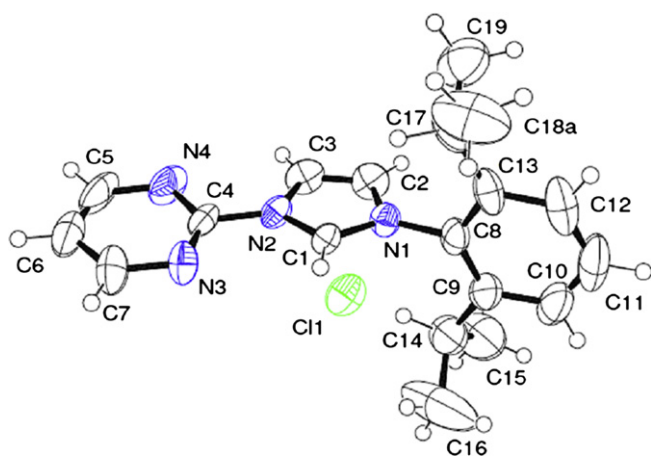


Fig. 1. ORTEP style plot of **1** in the solid state. Thermal ellipsoids are drawn at the 50% probability level. Selected bond lengths (Å) and angles (°): N2–C4 1.434(2), N2–C1 1.345(2), N1–C1 1.325(2), N1–C8 1.452(3), N1–C1–N2 108.8(2), C1–N1–C8 127.0(2), C1–N2–C4 125.4(2), C1–N2–C4–N3 –6.4(3), C1–N1–C8–C9 –84.9(2).

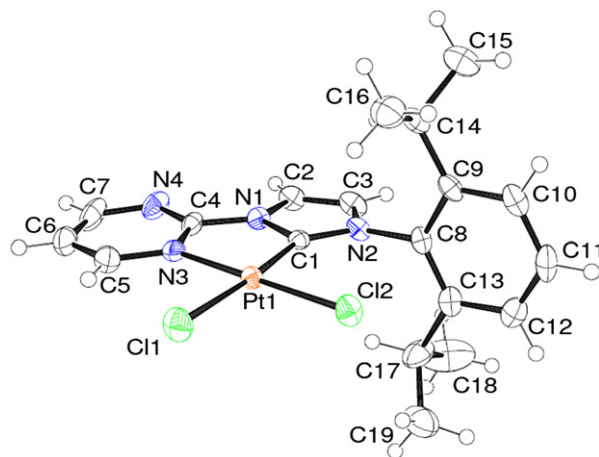


Fig. 3. ORTEP style plot of complexes **5** in the solid state. Thermal ellipsoids are drawn at the 50% probability level. Selected bond lengths (Å) and angles (°): Pt1–C1 1.946(4), Pt1–Cl1 2.339(1), Pt1–Cl2 2.269(1), Pt1–N3 2.029(3), C1–Pt1–N3 80.1(2), C1–Pt1–Cl1 173.7(1), C1–Pt1–Cl2 96.8(1), N3–Pt1–Cl2 176.5(1), C1–N1–C4–N3 0.0(5), C1–N2–C8–C9 –89.3(3).

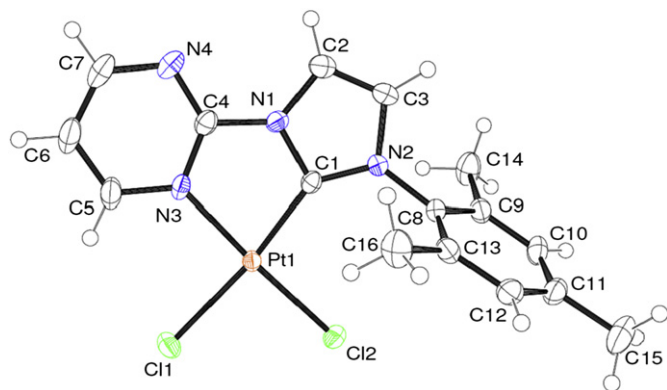
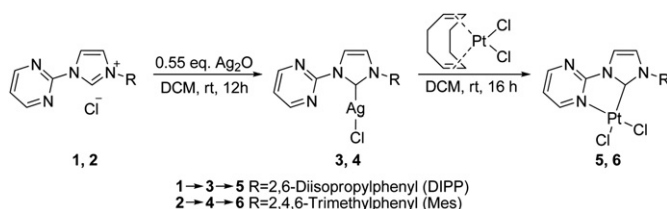


Fig. 4. ORTEP style plot of complexes **6***CH₃CN in the solid state. Thermal ellipsoids are drawn at the 50% probability level. One molecule acetonitrile has been omitted for clarity. Selected bond lengths (Å) and angles (°): Pt1–C1 1.949(2), Pt1–Cl1 2.351(1), Pt1–Cl2 2.299(1), Pt1–N3 2.029(2), C1–Pt1–N3 79.5(1), C1–Pt1–Cl1 172.2(1), C1–Pt1–Cl2 97.3(1), N3–Pt1–Cl2 176.7(1), C1–N1–C4–N3 –2.9(3), C1–N2–C8–C9 118.0(3).



Scheme 2. Synthesis of platinum(II) complexes **5** and **6**.

complexes **5** and **6***CH₃CN. In contrast, the pyrimidine ring deviates significantly in the silver complex **3**, indicating that no coordination from the pyrimidine N to Ag occurs. In the solid state structure of **1** the dihedral angle between the imidazol- and the pyrimidine heterocycle is 6.4°. The chloride counterion in the molecular structure of **1** is found quite close (2.437 Å) to the hydrogen atom bound to the C1 carbon atom, indicating a weak hydrogen bond

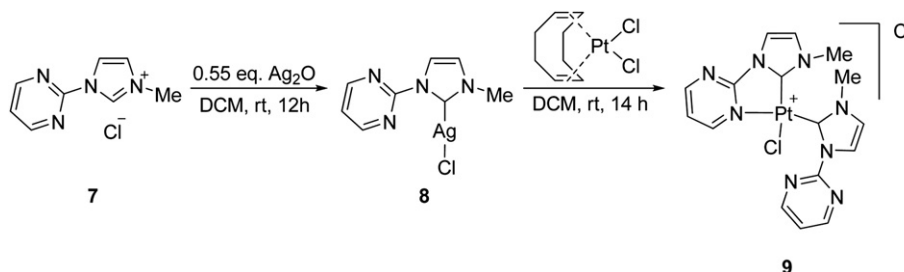
interaction to the certainly most acidic hydrogen atom of the molecule.

Attempts were made to synthesize platinum(II) complexes with aliphatic substituents (R = methyl, cyclohexyl) following the same protocol used for the synthesis of the complexes with aromatic substituents **5** and **6***CH₃CN, but led to different results. In case of the cyclohexyl substituent the [(pym)⁺(NHC-Cy)Pt^{II}Cl₂] complex **12** was obtained, while in case of the methyl substituent the 2:1 complex [(pym)⁺(NHC-Me)₂Pt^{II}Cl]Cl **9** was formed (Schemes 3 and 4). We had expected that the methyl substituted ligand might lead to a different structure as we had observed the formation of a [Pd(L)₂Cl][Pd(DMSO)Cl₃] complex for the corresponding palladium species with a methyl substituent [5]. Similar complexes for palladium and platinum are also known from the literature [20].

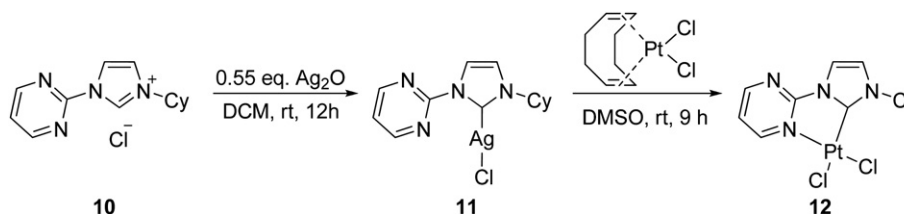
The structure of the previously reported complex [(pym)⁺(NHC-Me)₂Pt^{II}Cl] PF₆ differs from the solid state structure of **9** only by some degrees in the angles, but the bond lengths are quite similar. As already observed in the palladium complex [5], the two ligands in **9** lead to different signal sets and were also characterized as two different coordinating ligands in the solid state structure (Fig. 5). The quantitative formation (97% isolated yield) of **9** can be achieved by using an excess (2 eq.) of the silver precursor **8**.

As already mentioned the structure of complex **9** could be proven by X-Ray analysis, confirming the 2:1 coordination geometry that was assumed from the two different signal sets in the NMR-spectra. A similar structure containing a PF₆[−] counterion instead of Cl[−] was published earlier [20].

The analogous Pd(II) complexes have been shown to be active catalysts for the methane activation [5]. In order to investigate whether the Pt(II) complexes show a catalytic reaction as well, methane activation experiments were conducted with compounds **5**, **6** and **9**. Under the same reaction conditions as used before the complexes were stirred with K₂S₂O₈ as oxidant and a mixture of trifluoroacetic acid and its anhydride as solvent in a 160 mL Hastelloy C-2000 autoclave (Parr) under an atmosphere of 30 bars methane at 90 °C. Although no formation of platinum black could be observed and the platinum(II) complexes seem to be stable in concentrated trifluoroacetic acid, we were not able to observe any catalytic activity in the methane oxidation, a very unexpected result.



Scheme 3. Preparation and reaction of the silver complex **8** with dichlorido-cyclooctadiene-platinum(II).



Scheme 4. Synthesis of the cyclohexyl substituted Pt(II) complex **12**.

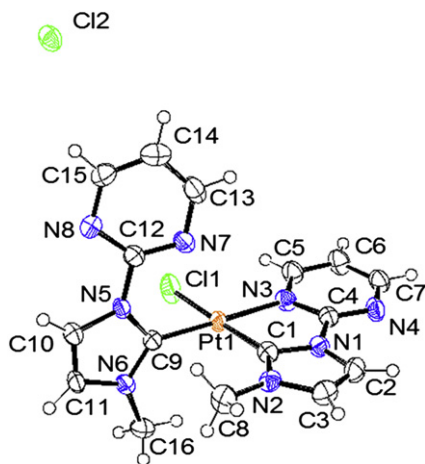


Fig. 5. ORTEP style plot of complex **9** in the solid state. Thermal ellipsoids are drawn at the 50% probability level. Selected bond lengths (Å) and angles (°): Pt1–C1 1.963(7), Pt1–C9 1.972(7), Pt1–Cl1 2.337(2), Pt1–N3 2.081(6), C1–Pt1–N3 79.4(3), C1–Pt1–Cl1 172.2(2), C1–Pt1–C9 98.8(3), C9–Pt1–N3 177.0(3), C1–N1–C4–N3 –3.6(9), C9–N5–C12–N7 –16.6(11).

3. Conclusion

4. Experimental section

¹H and ¹³C spectra were recorded on a Bruker AC 300 P or a Bruker DRX-500 spectrometer. Elemental analyses were performed by the microanalytical laboratory of our institute using an EuroVektor Euro EA-300 Elemental Analyzer. Melting points have been determined using a Wagner and Munz PolyTherm A system. Chemicals were supplied by Acros, Fluka and Aldrich, solvents were dried by standard procedures before use. 1-(2-pyrimidyl)-3-(2,6-diisopropylphenyl)imidazolium chloride [(pym)⁺(NHC-DIPP)]Cl **1**, 1-(2-pyrimidyl)-3-(2,4,6-trimethylphenyl)imidazolium chloride [(pym)⁺(NHC-Mes)]Cl **2**, 1-(2-pyrimidyl)-3-(2,6-diisopropylphenyl)imidazoline-2-ylidene silver(I) chloride [(pym)⁺(NHC-DIPP)AgCl] **3**, 1-(2-pyrimidyl)-3-(2,4,6-trimethylphenyl)-imidazoline-2-ylidene silver(I) chloride [(pym)⁺(NHC-Mes)AgCl] **4**, 1-(2-pyrimidyl)-3-(methyl)imidazolium chloride [(pym)⁺(NHC-Me)]Cl **7**, 1-(2-pyrimidyl)-3-(methyl)imidazol-2-ylidene silver(I) chloride [(pym)⁺(NHC-Me)AgCl] **8**, 1-(2-pyrimidyl)-3-(cyclohexyl)-imidazolium chloride [(pym)⁺(NHC-Cy)]Cl **10**, 1-(2-pyrimidyl)-3-(cyclohexyl)imidazol-2-ylidene silver(I) chloride [(pym)⁺(NHC-Cy)AgCl] **11**⁵ and dichlorido-cyclo-octadiene-platinum(II) [23] [(COD)Pt^{II}Cl₂] were prepared according to known procedures.

4.2. Synthesis of the metal complexes

0.27 g (0.7 mmol) silver carbene complex **3** and 0.25 g (0.7 mmol) dichloro-cyclooctadiene-platinum(II) were stirred in a Schlenk tube in 40 mL dichloromethane at room temperature for

16 h under exclusion of light. The resulting yellow solution was separated from the white residue by filtration and the solvent was evaporated in vacuo. The yellow precipitate was washed with diethylether and dried in vacuo. Yield: 0.19 g (80%). M.p. >350 °C. ¹H NMR (DMSO-d₆): 1.11 (d, *J* = 6.8 Hz, 6H, CH₃), 1.25 (d, *J* = 6.8 Hz, 6H, CH₃), 2.61 (sept, *J* = 6.9 Hz, 2H, CH), 7.28 (d, *J* = 7.7 Hz, 2H, m-H of ph), 7.47 (t, 1H, *J* = 7.7 Hz, p-H of ph), 7.76 (t, *J* = 5.4 Hz, 1H, p-H of pym), 7.81 (d, *J* = 2.1 Hz, 1H, NCH), 8.36 (d, *J* = 2.1 Hz, 1H, NCH), 9.15 (m, 1H, m-H pym), 9.76 (m, 1H, m-H pym). ¹³C NMR (DMSO-d₆) : δ = 22.9 (CH₃), 24.2 (CH₃), 27.9 (CH), 116.9 (p-CH of pym), 119.8 (NCH), 123.4 (m-CH of ph), 126.9 (NCH), 129.9 (p-CH of ph), 134.0 (ipso-C of ph), 143.7 (Carbene-C), 144.5 (o-C of ph), 156.4 (m-CH of pym), 157.6 (ipso-C of pym), 160.3 (m-CH of pym). Anal. Calcd for C₁₉H₂₂Cl₂N₄Pt: C 39.87%; H 3.87%; N 9.79% found C 40.21%; H 3.68%; N 9.95%.

4.2.2. Dichloro(1-(2-pyrimidyl)-3-(2,4,6-trimethylphenyl)imidazol-2-ylidene)platinum(II) $6^* \text{CH}_3\text{CN} [(pym)^\wedge(\text{NHC-Mes})\text{Pt}^{\text{II}}\text{Cl}_2]$

0.30 g (0.7 mmol) silver carbene complex **4** and 0.28 g (0.7 mmol) dichloro-cyclooctadiene-platinum(II) were stirred in a Schlenk tube in 40 mL dichloromethane at room temperature for 16 h under exclusion of light. The resulting yellow solution was separated from the white residue by filtration and the solvent was evaporated in vacuo. The yellow precipitate was washed with diethylether and dried in vacuo. Yield: 0.19 g (80%). M.p. >350 °C. ^1H NMR (DMSO- d_6): δ = 2.07 (s, 6H, o-CH₃), 2.31 (s, 3H, p-CH₃), 7.00 (s, 2H, m-H of ph), 7.62 (d, J = 1.8 Hz, 1H, NCH), 7.76 (t, J = 5.1 Hz, 1H, p-H of pym), 8.35 (d, J = 1.8 Hz, 1H, NCH), 9.15 (m, 1H, m-H of pym), 9.75 (m, 1H, m-H of pym). ^{13}C NMR (DMSO- d_6): δ = 17.3 (o-CH₃), 20.6 (p-CH₃), 117.3 (p-CH of pym), 119.8 (NCH), 125.6 (NCH), 128.4 (m-CH of ph), 134.1 (o-C of ph), 134.4 (p-C of ph), 138.3 (ipso-C of ph), 143.2 (Carbene-C), 156.5 (m-CH of pym), 157.6 (ipso-C pym), 160.3 (m-CH pym). Anal. Calcd for C₁₆H₁₆Cl₂N₄Pt: C 36.24%, H 3.04%, N 10.56% found C 36.02%, H 2.97%, N 10.48%.

4.2.3. Chlorobis(1-(2-pyrimidyl)-3-(methyl)imidazol-2-ylidene)platinum(II) chloride $[(\text{pym})^{\wedge}(\text{NHC-Me})_2\text{Pt}^{\text{II}}\text{Cl}]\text{Cl}$ **9**

0.08 g (0.3 mmol) of the silver complex **8** and 0.05 g (0.1 mmol) [Pt(COD)Cl₂] were dissolved in 5 mL DMSO. Under exclusion of light the reaction mixture is stirred in an inert gas atmosphere for 14 h. The resulting suspension was filtrated through a celite pad, the solvent was removed in vacuo. The residue was dissolved dichloromethane and precipitated by the addition of diethyl ether. The white product was filtrated and dried in vacuo. Yield: 0.07 g (97%). M.p. 200 °C. ¹H NMR (DMSO-d₆): δ = 3.09 (s, 3H, CH₃), 4.01 (s, 3H, CH₃), 7.61 (m, 2H, p-H of pym and NCH), 7.86 (m, 2H, p-H of pym and NCH), 8.16 (d, *J* = 2.2 Hz, 1H, NCH), 8.28 (d, *J* = 2.2 Hz, 1H, NCH), 8.89 (d, *J* = 4.9 Hz, 2H, m-H of pym), 9.22 (m, 1H, m-H of pym), 9.44 (m, 1H, m-H of pym). ¹³C NMR (DMSO-d₆): δ = 35.9 (CH₃), 40.4 (CH₃), 116.7 (p-CH of pym), 120.2 (p-CH of pym), 121.1 (NCH), 124.7 (NCH), 125.4 (NCH), 156.0 (m-CH of pym), 157.1 (ipso-C of pym), 159.2 (m-CH of pym), 161.8 (m-CH of pym). Anal. Calcd for C₁₆H₁₇Cl₂N₈Pt. 1.1 AgCl: C 25.79%, H 2.30%, N 15.04% found C 25.97%, H 2.04%, N 14.80%.

4.2.4. Dichloro(1-(2-pyrimidyl)-3-(cyclohexyl)imidazol-2-ylidene) platinum(II) [(pym)⁺(NHC-Cy) Pt^{II}Cl₂] **12**

0.20 g (0.5 mmol) of the silver complex **11** and 0.20 g (0.5 mmol) [Pt(COD)Cl₂] were dissolved in 5 mL DMSO. Under exclusion of light and inert atmosphere the reaction mixture is stirred for 9 h. The resulting suspension was filtrated through a celite pad, the solvent was removed in vacuo. The residue was dissolved in dichloromethane and precipitated by the addition of diethyl ether. The yellow product was filtrated and dried in vacuo. Yield: 0.09 g (35%). M.p. >350 °C. ¹H NMR (DMSO-d₆): δ = 1.23–1.96 (2m, 10H, CH₂ of cyc), 5.67 (m, 1H, NCH of cyc), 7.70 (t, *J* = 5.1 Hz, 1H, p-H of pym),

Table 1
Crystallographic data for complexes **1**, **3**, **5**, **6*CH₃CN** and **9**.

Compound	1	3	5	6*CH₃CN	9
Empirical formula	C ₁₉ H ₂₃ ClN ₄	C ₁₉ H ₂₂ AgClN ₄	C ₁₉ H ₂₂ Cl ₂ N ₄ Pt	C ₁₆ H ₁₆ Cl ₂ N ₄ Pt *C ₂ H ₃ N	C ₁₆ H ₁₆ Cl ₂ N ₈ Pt
Formula weight	342.86	449.73	572.40	571.37	586.36
Temperature	198(2) K	198(2) K	198(2) K	198(2) K	198(2) K
Wavelength	0.71073 Å	0.71073 Å	0.71073 Å	0.71073 Å	0.71073 Å
Crystal system	Orthorhombic	Monoclinic	Monoclinic	Monoclinic	Triclinic
Space group	P n a 21	P21/c	P21/c	P21/c	P -1
Unit cell dimensions	<i>a</i> = 16.269(1) Å <i>b</i> = 11.977(1) Å <i>c</i> = 9.828(1) Å α = 90° β = 90° γ = 90°	<i>a</i> = 11.154(1) Å <i>b</i> = 14.918(1) Å <i>c</i> = 15.541(1) Å α = 90° β = 127.88(1)° γ = 90°	<i>a</i> = 8.887(1) Å <i>b</i> = 17.872(2) Å <i>c</i> = 14.497(1) Å α = 90° β = 120.28(1)° γ = 90°	<i>a</i> = 10.486(1) Å <i>b</i> = 14.026(1) Å <i>c</i> = 13.824(1) Å α = 90° β = 105.96(1)° γ = 90°	<i>a</i> = 7.057(2) Å <i>b</i> = 11.143(4) Å <i>c</i> = 12.544(3) Å α = 99.52(3)° β = 99.59(2)° γ = 90.06(3)°
Volume	1915.0(3) Å ³	2041.1(2) Å ³	1988.5(3) Å ³	1954.8(3) Å ³	958.8(4) Å ³
Z	4	4	4	4	2
Absorption coefficient	0.207 mm ⁻¹	1.127 mm ⁻¹	7.336 mm ⁻¹	7.463 mm ⁻¹	7.615 mm ⁻¹
F(000)	728	912	1104	1096	560
Crystal size [mm ³]	0.39 × 0.32 × 0.27	0.60 × 0.50 × 0.23	0.38 × 0.27 × 0.06	0.51 × 0.31 × 0.15	0.17 × 0.08 × 0.08
Theta range for data collection	4.85–26.40°	4.83–26.40°	4.84–26.40°	4.81–26.39°	4.80–26.40°
Reflections collected	16,107	24,244	20,941	24,487	17,218
Independent reflections	3755 [<i>R</i> (int) = 0.0391]	4154 [<i>R</i> (int) = 0.0252]	4046 [<i>R</i> (int) = 0.0607]	3969 [<i>R</i> (int) = 0.0277]	3905 [<i>R</i> (int) = 0.0843]
Max. and min. transmission	0.9463 and 0.9234	0.7754 and 0.5458	0.6406 and 0.1598	0.4087 and 0.1141	0.5706 and 0.3593
Data/restraints/parameters	3755/1/222	4154/0/226	4046/0/239	3969/0/239	3905/0/246
Goodness-of-fit on F ²	1.109	1.288	1.040	1.331	1.101
Final <i>R</i> indices	<i>R</i> ₁ = 0.0355, [<i>I</i> > 2σ(<i>I</i>)] <i>wR</i> ₂ = 0.0834	<i>R</i> ₁ = 0.0212, <i>wR</i> ₂ = 0.0522	<i>R</i> ₁ = 0.0252, <i>wR</i> ₂ = 0.0466	<i>R</i> ₁ = 0.0171, <i>wR</i> ₂ = 0.0434	<i>R</i> ₁ = 0.0412, <i>wR</i> ₂ = 0.0906
<i>R</i> indices (all data)	<i>R</i> ₁ = 0.0518, <i>wR</i> ₂ = 0.0905	<i>R</i> ₁ = 0.0318, <i>wR</i> ₂ = 0.0557	<i>R</i> ₁ = 0.0454, <i>wR</i> ₂ = 0.0514	<i>R</i> ₁ = 0.0205, <i>wR</i> ₂ = 0.0449	<i>R</i> ₁ = 0.0567, <i>wR</i> ₂ = 0.0968
Largest diff. peak and hole	0.122 and –0.137 e Å ⁻³	0.446 and –0.423 e Å ⁻³	0.605 and –0.635 e Å ⁻³	0.578 and –1.358 e Å ⁻³	1.798 and –1.317 e Å ⁻³

7.89 (d, *J* = 2.4 Hz, 1H, NCH), 8.11 (d, *J* = 2.3 Hz, 1H, NCH), 9.09 (m, 1H, m-H of pym), 9.78 (m, 1H, m-H of pym). ¹³C NMR (DMSO-d₆): δ = 24.4 (p-CH₂ of cyc), 25.0 (m-CH₂ of cyc), 32.3 (o-CH₂ of cyc), 56.9 (NCH of cyc), 117.1 (p-CH of pym), 119.5 (NCH), 120.9 (NCH), 140.1 (Carbene-C), 156.4 (m-CH of pym), 157.6 (ipso-C pym), 160.4 (m-CH pym). Anal. Calcd for C₁₃H₁₆Cl₂N₄Pt: C 31.59%, H 3.26%, N 11.34% found C 31.76%, H 3.13%, N 11.14%.

4.3. Solid-state structure determination of compounds **1**, **3**, **5**, **6*CH₃CN** and **9**

Preliminary examination and data collection were carried out on an area detecting system (Kappa-CCD; Nonius) at the window of a sealed X-ray tube (Nonius, FR590) and graphite monochromated Mo K α radiation (λ = 0.71073 Å). The reflections were integrated. Raw data were corrected for Lorentz and polarization and, arising from the scaling procedure, for latent decay. An absorption correction was applied using SADABS [24]. After merging, the independent reflections were all used to refine the structures. The structures were solved by a combination of direct methods and difference Fourier synthesis. All non-hydrogen atoms were refined with anisotropic displacement parameters. All hydrogen atoms were placed in calculated positions and refined using the riding model. Full-matrix least-squares refinements were carried out by minimizing $\sum w(F_o^2 - F_c^2)^2$. Details of the structure determinations are given in Table 1. Neutral atom scattering factors for all atoms and anomalous dispersion corrections for the non-hydrogen atoms were taken from the *International Tables for Crystallography* [25]. All calculations were performed with the SHELXL-97 package [26] and the programs COLLECT [27], DIRAX [28], EVALCCD [29], SIR-92 [30], SADABS [24], ORTEP III [31] and PLATON [32].

Appendix A. Supplementary material

CCDC-856642 (**1**), -856643 (**3**), -856644 (**5**), -856645 (**6*CH₃CN**) and -856646 (**9**); contains the supplementary crystallographic data

for this paper. These data can be obtained free of charge from The Cambridge Crystallographic Data Centre via www.ccdc.cam.ac.uk/data_request/cif.

References

- [1] R.A. Periana, D.J. Taube, S. Gamble, H. Taube, T. Satoh, H. Fujii, *Science* 280 (1998) 560–564.
- [2] J. Kua, X. Xu, R.A. Periana, W.A. Goddard III, *Organometallics* 21 (2002) 511–525.
- [3] M. Ahlquist, R.A. Periana, W.A. Goddard III, *Chem. Commun.* (2009) 2373–2375.
- [4] M. Muehlhofer, T. Strassner, W.A. Herrmann, *Angew. Chem. Int. Ed.* 41 (2002) 1745–1747.
- [5] D. Meyer, M.A. Taige, A. Zeller, K. Hohlfield, S. Ahrens, T. Strassner, *Organometallics* 28 (2009) 2142–2149.
- [6] A. Zeller, Ph. D. thesis. Technische Universität München, 2006.
- [7] T. Strassner, S. Ahrens, A. Zeller, *WO 2006058535*, 2006.
- [8] S. Warsink, I.H. Chang, J.J. Weigand, P. Hauwert, J.-T. Chen, C.J. Elsevier, *Organometallics* 29 (2010) 4555–4561.
- [9] B. Liu, B. Liu, Y. Zhou, W. Chen, *Organometallics* 29 (2010) 1457–1464.
- [10] D. Gnanamgari, E.L.O. Sauer, N.D. Schley, C. Butler, C.D. Incavito, R.H. Crabtree, *Organometallics* 28 (2009) 321–325.
- [11] Z. Xi, B. Liu, C. Lu, W. Chen, *Dalton Trans.* (2009) 7008–7014.
- [12] X. Zhang, Q. Xia, W. Chen, *Dalton Trans.* (2009) 7045–7054.
- [13] X. Zhang, B. Liu, A. Liu, W. Xie, W. Chen, *Organometallics* 28 (2009) 1336–1349.
- [14] J. Ye, W. Chen, D. Wang, *Dalton Trans.* (2008) 4015–4022.
- [15] C. Chen, H. Qiu, W. Chen, D. Wang, *J. Organomet. Chem.* 693 (2008) 3273–3280.
- [16] K.-M. Lee, J.C.C. Chen, C.-J. Huang, I.J.B. Lin, *CrystEngComm* 9 (2007) 278–281.
- [17] K.-M. Lee, J.C.C. Chen, I.J.B. Lin, *J. Organomet. Chem.* 617–618 (2001) 364–375.
- [18] B. Liu, Q. Xia, W. Chen, *Angew. Chem. Int. Ed.* 48 (2009) 5513–5516.
- [19] B. Liu, Y. Zhang, D. Xu, W. Chen, *Chem. Commun.* 47 (2011) 2883–2885.
- [20] C. Lu, S. Gu, W. Chen, H. Qiu, *Dalton Trans.* 39 (2010) 4198–4204.
- [21] S. Ahrens, T. Strassner, *Inorg. Chim. Acta* 359 (2006) 4789–4796.
- [22] S. Ahrens, E. Herdtweck, S. Goutal, T. Strassner, *Eur. J. Inorg. Chem.* (2006) 1268–1274.
- [23] D. Drew, J.R. Doyle, *Inorg. Synth.* 28 (1990) 346–349 Reagents Transition Met. Complex Organomet. Synth.
- [24] G.M. Sheldrick, SADABS, Version 2.10, University of Goettingen, Goettingen, Germany, 2003.
- [25] A.J.C. Wilson, *International Tables for Crystallography*, Kluwer Academic Publisher, Dordrecht, The Netherlands, 1992.
- [26] G.M. Sheldrick, SHELXL-97: Program for the Refinement of Structures, University of Göttingen, Göttingen, Germany, 1997.
- [27] Nonius, Data Collection Software for Nonius Kappa CCD Delft (2001) The Netherlands.
- [28] A.J.M. Duisenberg, *J. Appl. Crystallogr.* 25 (1992) 92–96.

- [29] A.J.M. Duisenberg, R.W.W. Hooft, A.M.M. Schreurs, J. Kroon, J. Appl. Crystallogr. 33 (2000) 893–898.
- [30] A. Altomare, G. Cascarano, C. Giacovazzo, A. Guagliardi, M.C. Burla, G. Polidori, M. Camalli, J. Appl. Crystallogr. 27 (1994) 435–436.
- [31] M.N. Burnett, K.J. Carroll, ORTEP-III: Oak Ridge Thermal Ellipsoid Plot Program for Crystal Structure Illustrations, Oak Ridge National Laboratory, 1996, Report ORNL-6895.
- [32] A.L. Spek, PLATON, Utrecht University, Utrecht, The Netherlands, 2001.